Journal of Solid State Chemistry **168,** 18–27 (2002)
doi:10.1006/jssc.2002.9670

Equiatomic Rare Earth (*Ln*) Transition Metal Antimonides *Ln*T Sb (*T*=Rh, Ir) and Bismuthides *Ln*T Bi (*T*=Rh, Ni, Pd, Pt)

Martin G. Haase, Tobias Schmidt, Carolin G. Richter, Helga Block, and Wolfgang Jeitschko[1]

Anorganisch-Chemisches Institut, Universität Münster, Wilhelm-Klemm-Strasse 8, D-48149 Münster, Germany

Received February 25, 2002; in revised form May 13, 2002; accepted May 28, 2002

Thirty-eight new ternary equiatomic antimonides and bismuthides were prepared by reaction of the elemental components at high temperatures, and the structures of four compounds were refined from single-crystal X-ray data. The antimonides *Ln*RhSb (*Ln* = Sm, Gd–Tm) and *Ln*IrSb (*Ln* = La–Nd, Sm, Gd–Tm) crystallize with the orthorhombic TiNiSi-type structure, which was refined for TbRhSb ($a = 713.3(2)$ pm, $b = 452.0(1)$ pm, $c = 778.8(2)$ pm, $R = 0.016$ for 306 structure factors and 20 variable parameters) and SmIrSb ($a = 722.4(2)$ pm, $b = 452.9(1)$ pm, $c = 786.1(2)$ pm, $R = 0.023$ for 559 F values and 20 variables). The bismuthides *Ln*RhBi (*Ln* = Pr–Sm) also crystallize with TiNiSi-type structure which was refined for SmRhBi ($a = 728.0(2)$ pm, $b = 467.9(1)$ pm, $c = 795.7(2)$ pm, $R = 0.037$ for 481 F values and 20 variables). The hexagonal ZrNiAl-type structure was established for the compounds *Ln*RhBi (*Ln* = Gd–Er) through a structure refinement of DyRhBi ($a = 757.9(2)$ pm, $c = 392.6(1)$ pm, $R = 0.026$ for 423 F values and 14 variables). The bismuthides *Ln*NiBi (*Ln* = Pr, Nd, Sm, Tb, Ho, Er), ScPdBi, *Ln*PdBi (*Ln* = La, Er, Tm, Lu), and LaPtBi are isotypic with cubic MgAgAs. The atomic order for these equiatomic ternary bismuthides was determined for PrNiBi and LaPtBi from X-ray powder data. The structural chemistry of these compounds is briefly discussed.

INTRODUCTION

A large number of equiatomic ternary compounds have been reported with compositions ATM, where A are large electropositive elements, e.g., alkaline earth elements, the rare earth elements, and early transition metals; the T components are late transition metals; and M stands for main group metals or metalloids, mainly aluminum, silicon, phosphorus, and their homologues. Villars (1) and Hovestreydt (2) have reviewed the literature on the structural chemistry of these compounds, which frequently crystallize with very simple structure types. Many of these remain to be discovered and characterized. Some of them may have interesting physical properties. Those containing cerium, europium, or ytterbium are of interest because of their potential for mixed or intermediate valence behavior. The crystallographic and physical properties of equiatomic compounds with europium and ytterbium have been reviewed recently (3, 4). In the present paper we report on ternary rare earth transition metal antimonides and bismuthides.

Known antimonides of this composition include the series *Ln*RhSb (*Ln* = La–Nd) with the orthorhombic TiNiSi-type structure (5, 6). The nickel-containing compounds of the small rare earth elements ScNiSb, YNiSb, and the series *Ln*NiSb (*Ln* = Gd–Lu) crystallize with the cubic MgAgAs-type structure (7, 8). For the corresponding compounds with the large early rare earth elements *Ln*NiSb (*Ln* = La–Nd, Sm, Gd) a hexagonal ZrBeSi- (sometimes also called ordered Ni_2In-) type structure has been established (8, 9). The homologous series *Ln*PdSb with *Ln* = La–Nd, Sm, Gd, Tb is reported to crystallize with the hexagonal (disordered) $CaIn_2$-type structure (10, 11). For *Ln* = Y, Dy–Lu the cubic MgAgAs-type structure was observed (10–12); while the europium compound EuPdSb has the orthorhombic TiNiSi-type structure (10). The platinum-containing compounds ScPtSb, YPtSb, and the series *Ln*PtSb (*Ln* = Gd–Lu) crystallize with the cubic MgAgAs-type structure (7). For the analogous compounds with the large early rare earth elements *Ln*PtSb (*Ln* = La–Nd) a (disordered) $CaIn_2$-type structure has been reported on the basis of X-ray powder data (13), while a single-crystal study of the neodymium compound NdPtSb revealed an ordered distribution for the platinum and antimony atoms (14). For the europium compound EuPtSb the orthorhombic TiNiSi-type structure (15) has been established.

Of the corresponding bismuthides the series *R*NiBi (*R* = Sc, Y, Gd, Dy, Tm, Lu), *R*PdBi (*R* = Y, Ce–Nd, Sm, Gd–Ho, Yb), and *R*PtBi (*R* = Y, Ce–Nd, Sm, Gd–Lu) are

[1]To whom correspondence should be addressed. Fax: +49(0)25183-33120. E-mail: jeitsch@uni-muenster.de.

0022-4596/02 $35.00

reported to crystallize with the cubic MgAgAs-type structure (7, 16–18). The rhodium-containing compounds cyrstallize with the orthorhombic TiNiSi-type structure (19).

The present paper reports on new ternary equiatomic rare earth antimonides and bismuthides with mainly the transition metals rhodium, iridium, nickel, and palladium as third components. Some preliminary accounts of this work have been given at conferences (20–22).

SAMPLE PREPARATION AND LATTICE CONSTANTS

The samples were prepared by reaction of the elemental components. Starting materials were chips of scandium and yttrium (Kelpin), ingots of the rare earth elements (Kelpin), powders of rhodium (Merck), nickel (Merck), palladium (Heraeus), platinum (Heraeus), and shots of antimony (Johnson Matthey) and bismuth (Chempur), all with nominal purities >99.9%.

The antimonides *Ln*RhSb (*Ln* = La–Nd, Sm, Gd–Tm) and *Ln*IrSb (*Ln* = La–Nd, Sm, Gd–Tm) were prepared from cold-pressed pellets of the elements by arc-melting from each side. The resulting ingots were sealed in silica tubes under vacuum and annealed for 1 h just below their melting temperatures in a high-frequency furnace to enhance their cyrstallinity.

For the preparation of the bismuthides *Ln*RhBi (*Ln* = Pr, Nd, Sm, Gd–Er) a mixture of the elements with an excess of bismuth (ca. 10%, to compensate the loss during the arc-melting) was pressed to pellets and arc-melted from each side. The resulting ingots were sealed under vacuum into silica tubes and annealed for 7 days at 900°C in order to homogenize the samples.

The bismuthides ScPdBi and *Ln*PdBi (*Ln* = La, Pr, Sm, Tb, Er, Tm, and Lu) were prepared by annealing (600°C, 3 h) cold-pressed pellets of the components in evacuated silica tubes. The reaction products were subsequently melted in a high-frequency furnace and cooled to room temperature within 1 min.

The nickel- and platinum-containing compounds *Ln*NiBi (*Ln* = Pr, Nd, Sm, Tb, Ho, Er), YPtBi, and *Ln*PtBi (*Ln* = La, Tb, Tm–Lu) were prepared by arc-melting the elements in the ideal atomic ratio 1:1:1. The resulting ingots were then sealed under vacuum into silica tubes and annealed for 7 days at 800°C, followed by quenching in air.

The products were generally obtained in well-cyrstallized form with black color. They are stable in air for long periods of time. Energy dispersive X-ray flourescence analyses of the samples in a scanning electron microscope did not show any impurity elements heavier than sodium.

All samples were characterized by their Guinier powder patterns with Cu$K\alpha_1$ radiation and α-quartz ($a = 491.30$ pm, $c = 540.46$ pm) as an internal standard. To facilitate the proper assignment of indices, the experimental patterns were compared with the ones calculated (23) using the positional parameters obtained from single-crystal investigations. The lattice parameters were obtained by least-squares fits. They are listed in Tables 1 and 2. For those compounds which have also been characterized by other research groups we also list the lattice parameters reported in the literature.

STRUCTURE REFINEMENTS

Single crystals of TbRhSb, SmIrSb, SmRhBi, and DyRhBi were isolated from the crushed annealed samples. They were investigated with Buerger precession and Weissenberg cameras to establish their symmetry and suitability for the intensity data collections. The intensity data were recorded on a four-circle diffractometer (CAD4) using graphite-monochromated Mo$K\alpha$ radiation, a scintillation counter with pulse-height discrimination, $\theta/2\theta$ scans, and background counts at both ends of each scan. Absorption corrections were made from psi scan data. Further details are summarized in Table 3.

TABLE 1
Lattice Parameters of Antimonides with the Orthorhombic TiNiSi-Type Structure[a]

Compound	a (pm)	b (pm)	c (pm)	V (nm^3)	Reference
LaRhSb	754.7(4)	464.6(4)	789.8(4)	0.2769	5
LaRhSb	754.1(2)	462.1(2)	792.6(3)	0.2762	this work
CeRhSb	741.6(4)	460.9(4)	784.6(4)	0.2682	5
CeRhSb	741.50(3)	461.85(2)	785.70(3)	0.2691	6
CeRhSb	740.8(1)	460.5(1)	786.1(2)	0.2682	this work
PrRhSb	739.1(4)	459.6(4)	784.8(4)	0.2666	5
PrRhSb	738.4(2)	458.5(1)	783.8(2)	0.2654	this work
NdRhSb	732.9(4)	458.4(4)	783.8(4)	0.2633	5
NdRhSb	730.7(2)	459.3(1)	786.0(2)	0.2638	this work
SmRhSb	724.4(2)	452.0(2)	786.9(2)	0.2577	this work
GdRhSb	718.2(2)	450.7(2)	785.4(2)	0.2542	this work
TbRhSb	714.3(1)	451.8(2)	780.2(3)	0.2518	this work
DyRhSb	710.5(1)	449.9(1)	778.6(1)	0.2489	this work
HoRhSb	708.2(1)	446.8(1)	778.6(2)	0.2464	this work
ErRhSb	706.0(2)	446.9(1)	777.5(2)	0.2453	this work
TmRhSb	701.9(2)	448.5(1)	775.7(2)	0.2442	this work
LaIrSb	756.3(1)	459.8(1)	797.8(2)	0.2774	this work
CeIrSb	736.0(1)	457.8(1)	793.1(2)	0.2672	this work
PrIrSb	731.8(2)	457.8(2)	793.8(2)	0.2659	this work
NdIrSb	732.1(2)	456.4(2)	791.1(2)	0.2643	this work
SmIrSb	725.3(2)	455.3(1)	787.7(2)	0.2601	this work
GdIrSb	720.2(2)	452.4(2)	786.8(2)	0.2564	this work
TbIrSb	719.1(2)	451.8(2)	780.4(4)	0.2535	this work
DyIrSb	712.3(2)	450.2(2)	781.3(2)	0.2505	this work
HoIrSb	711.6(2)	448.1(1)	777.2(2)	0.2478	this work
ErIrSb	706.2(1)	450.1(1)	775.3(2)	0.2464	this work
TmIrSb	704.8(2)	448.7(2)	776.8(3)	0.2457	this work

[a] Standard deviations in the positions of the least significant digits are given in parentheses throughout the paper.

TABLE 2
Lattice Parameters of Bismuthides with Orthorhombic TiNiSi-, Hexagonal ZrNiAl-, and Cubic MgAgAs-Type Structure

Compound	a (pm)	b (pm)	c (pm)	V (nm^3)	Reference
LaRhBi	758.8	477.2	808.7	0.2928	19
CeRhBi	743.8	474.0	798.5	0.2815	19
CeRhBi	746.48	471.73	797.15	0.2807	6
PrRhBi	741.7(2)	472.8(1)	800.9(2)	0.2809	this work
NdRhBi	737.7(2)	471.0(1)	800.8(2)	0.2782	this work
SmRhBi	729.1(2)	469.1(1)	797.1(2)	0.2726	this work
GdRhBi	761.6(1)	—	396.9(1)	0.1994	this work
TbRhBi	759.6(2)	—	393.8(1)	0.1968	this work
DyRhBi	758.3(2)	—	391.9(1)	0.1952	this work
HoRhBi	757.6(1)	—	391.2(1)	0.1945	this work
ErRhBi	756.5(2)	—	389.2(1)	0.1929	this work
ScNiBi	619.1	—	—	0.2373	7
YNiBi	641.1	—	—	0.2635	7
PrNiBi	651.2(2)	—	—	0.2761	this work
NdNiBi	647.9(2)	—	—	0.2720	this work
SmNiBi	643.3(2)	—	—	0.2662	this work
GdNiBi	643.5	—	—	0.2665	7
TbNiBi	641.9(1)	—	—	0.2645	this work
DyNiBi	641.5	—	—	0.2640	7
HoNiBi	639.1(1)	—	—	0.2610	this work
ErNiBi	637.5(1)	—	—	0.2591	this work
TmNiBi	636.8	—	—	0.2582	7
LuNiBi	634.0	—	—	0.2548	7
ScPdBi	643.5(1)	—	—	0.2665	this work
YPdBi	664.0	—	—	0.2928	16
LaPdBi	682.5(1)	—	—	0.3179	this work
CePdBi	683.0	—	—	0.3186	16
PrPdBi	679.7(1)	—	—	0.3140	this work
PrPdBi	679.4	—	—	0.3136	17
NdPdBi	677.8	—	—	0.3114	16
SmPdBi	671.9(2)	—	—	0.3033	this work
SmPdBi	675.7	—	—	0.3085	17
GdPdBi	669.8	—	—	0.3005	16
TbPdBi	666.0(1)	—	—	0.2955	this work
TbPdBi	665.0	—	—	0.2941	17
DyPdBi	664.3	—	—	0.2932	16
HoPdBi	661.0	—	—	0.2888	16
ErPdBi	659.4(1)	—	—	0.2867	this work
TmPdBi	656.4(1)	—	—	0.2828	this work
YbPdBi	659.2	—	—	0.2865	16
LuPdBi	656.6(1)	—	—	0.2831	this work
YPtBi	664.0(1)	—	—	0.2928	this work
YPtBi[a]	666	—	—	0.2954	18
LaPtBi	682.9(1)	—	—	0.3185	this work
CePtBi	677.9(1)	—	—	0.3116	this work
CePtBi	684	—	—	0.3200	18
PrPtBi	678	—	—	0.3117	18
NdPtBi	676	—	—	0.3089	18
SmPtBi	674	—	—	0.3062	18
GdPtBi	668.0	—	—	0.2981	7
TbPtBi	666.2(1)	—	—	0.2957	this work
TbPtBi[a]	666	—	—	0.2954	18
DyPtBi	664.4	—	—	0.2933	7
HoPtBi	663.1	—	—	0.2916	7
ErPtBi	661.6	—	—	0.2896	7
TmPtBi	658.8(1)	—	—	0.2859	this work
TmPtBi[a]	660.1	—	—	0.2876	18
YbPtBi	658.4(1)	—	—	0.2855	this work
YbPtBi[a]	660	—	—	0.2875	18
LuPtBi	657.4(1)	—	—	0.2840	this work
LuPtBi[a]	659	—	—	0.2862	18

[a] The data of Ref. (18) have been extracted by us from a plot.

The structures were solved and refined using the program systems SDP (24) and SHELXL-97 (25). The structures of TbRhSb, SmIrSb, and SmRhBi turned out to correspond to the well-known orthorhombic TiNiSi (Co_2Si, anti-$PbCl_2$) type, while DyRhBi was found to be isotypic with hexagonal ZrNiAl (ordered Fe_2P-type). The structures were refined by full-matrix least-squares fits using atomic scattering factors, corrected for anomalous dispersion as provided by the programs. The weighting schemes accounted for the counting statistics and variables correcting for isotropic secondary extinction were optimized as least-squares parameters.

As checks for the correct compositions and the correct atom assignments we refined the occupancy parameters of all atoms of the four structures together with anisotropy displacement parameters, while the scale factors were fixed at the previously obtained values. These calculations were carried out with the least-squares program provided by the SDP system (24). As can be seen from Table 4, the resulting occupancy values were all very close to unity (100%). The only exception was the occupancy parameter for the Rh2 position of DyRhBi with a value of 95.1% and a standard deviation of 0.6%. Thus, this value was off the ideal occupancy by 8σ. Nevertheless, we assumed for the final refinement cycles the ideal occupancy values for all atomic positions of all four structure refinements.

The bismuthide DyRhBi crystallizes with the non-centrosymmetric space group $P\bar{6}2m$. Thus, one has to check for the correct handedness of the particular crystal used for the X-ray data collection. With the SHELXL-97 program system (25) this is evaluated with the Flack parameter (27, 28), which clearly indicated that (somewhat by accident) we had arrived at the correct handedness for our crystal. For typical solid-state compounds one can expect that a polycrystalline sample consists of approximately equal amounts of left- and right-handed crystals.

The conventional residuals R (on F values $> 2\sigma(F)$) of the four structure refinements are all smaller than 0.030 with the exception of $R = 0.037$ obtained for the refinement of the structure of SmRhBi. This structure also resulted in the highest residual electron densities in the difference Fourier analysis with $8.2\,e/Å^3$ as the highest peak. However, these peaks were all very close to fully occupied atomic sites and therefore not suited for additional atomic positions.

The cubic MgAgAs-type structure (29) of the ternary bismuthides LnTBi (T = Ni, Pd, Pt) listed in Table 2 is most simple and has only the lattice parameter as variable. Nevertheless, not counting equivalent permutations, it has three different possibilities for the occupancy of the three atomic sites, as has been discussed with more detail for the structure of NbFeSb (30). With PrNiBi as example we have tried all three possibilities and we obtained good agreement between observed and calculated (23) X-ray powder

TABLE 3
Crystal Data for the Compounds TbRhSb, SmIrSb, SmRhBi, and DyRhBi

Compound	TbRhSb,	SmIrSb,	SmRhBi,	DyRhBi
Space group	*Pnma* (No. 62)	*Pnma* (No. 62)	*Pnma* (No. 62)	$P\bar{6}2\,m$ (No. 189)
Structure type	TiNiSi	TiNiSi	TiNiSi	ZrNiAl
Pearson symbol	*oP*12	*oP*12	*oP*12	*h*P9
Lattice parameters (single crystals)				
a (pm)	713.3(2)	722.4(2)	728.0(2)	757.9(2)
b (pm)	452.0(1)	452.9(1)	467.9(1)	—
c (pm)	778.8(2)	786.1(2)	795.7(2)	392.6(1)
V (nm^3)	0.2511	0.2572	0.2710	0.1953
Formula units/cell, *Z*	4	4	4	3
Formula mass	383.6	464.4	462.3	474.4
Calculated density (g/cm^3)	10.15	11.99	11.33	12.10
Crystal dimensions (μm)	$40 \times 40 \times 60$	$25 \times 25 \times 90$	$10 \times 60 \times 95$	$25 \times 43 \times 125$
Scans up to 2θ	60°	70°	70°	80°
Range in *hkl*	±10, 0–6, ±10	±11, 0–7, ±12	±11, ±7, ±12	±13, ±13, ±7
Transmission (highest/lowest)	1.72	1.32	2.83	1.75
Total no. of reflections	2080	2247	4143	4218
Unique reflections	406	628	652	488
Internal residual, R_i (F^2)	0.041	0.029	0.127	0.083
Reflections with $I_o > 2\sigma(I_o)$	306	559	481	423
No. of variables	20	20	20	14
Maximal residual peak/hole ($e/Å^3$)	2.1/−1.5	2.4/−2.9	8.2/−5.2	2.5/−3.3
Conventional residual, R ($F > 2\sigma$)	0.016	0.023	0.037	0.026
Weighted residual, R_w (all F^2)	0.034	0.051	0.094	0.052

intensities only for the following occupancies in space group $F\bar{4}3\,m$ (No. 216): Pr on 4*b*) $\frac{1}{2}, \frac{1}{2}, \frac{1}{2}$; Ni on 4*c*) $\frac{1}{4}, \frac{1}{4}, \frac{1}{4}$; Bi on 4*a*) 0, 0, 0. This is the analogous occupancy as observed for ZrCoBi (30) and ZrNiSn (31). It should be mentioned that with $ZrNi_2Sn$ the system zirconium–nickel–tin also contains the closely related cubic "filled" MgAgAs structure, i.e., the cubic $MnCu_2Al$- (Heusler-) type structure (31). For that reason—using the example LaPtBi

TABLE 4
Atomic Parameters of the Ternary Antimonides TbRhSb, SmIrSb, SmRhBi, and DyRhBi[a]

Atom		Occupancy	*x*	*y*	*z*	*B*
TbRhSb	*Pnma*					
Tb	4*c*	1.000(1)	0.00716(4)	$\frac{1}{4}$	0.70260(4)	0.60(1)
Rh	4*c*	0.987(2)	0.30629(7)	$\frac{1}{4}$	0.41865(6)	0.78(1)
Sb	4*c*	1.002(1)	0.19693(5)	$\frac{1}{4}$	0.09161(5)	0.58(1)
SmIrSb	*Pnma*					
Sm	4*c*	0.998(1)	0.01052(4)	$\frac{1}{4}$	0.69531(4)	0.49(1)
Ir	4*c*	0.999(1)	0.29536(3)	$\frac{1}{4}$	0.41206(3)	0.48(1)
Sb	4*c*	1.006(2)	0.18070(5)	$\frac{1}{4}$	0.08776(4)	0.41(1)
SmRhBi	*Pnma*					
Sm	4*c*	0.998(3)	0.01016(9)	$\frac{1}{4}$	0.70116(9)	0.62(1)
Rh	4*c*	0.998(3)	0.2933(1)	$\frac{1}{4}$	0.4201(1)	0.75(2)
Bi	4*c*	1.001(2)	0.19029(6)	$\frac{1}{4}$	0.09053(7)	0.60(1)
DyRhBi	$P\bar{6}2m$					
Dy	3*f*	0.996(2)	0.60163(7)	0	0	0.64(1)
Rh1	2*d*	1.027(4)	$\frac{1}{3}$	$\frac{2}{3}$	$\frac{1}{2}$	0.92(2)
Rh2	1*a*	0.951(6)	0	0	0	0.60(2)
Bi	3*g*	1.001(3)	0.26746(5)	0	$\frac{1}{2}$	0.50(1)

[a] The positional parameters were standardized with the program STRUCTURE TIDY (26). The occupancy parameters were obtained in separate refinement cycles. In the final cycles the ideal occupancy parameters were used. The last column contains the equivalent isotropic *B* values (in units of $10^4\,pm^2$).

and the hypothetical compound "$LaPt_2Bi$"—we have also calculated the powder patterns for these two structure types (MgAgAs and $MnCu_2Al$). They differ greatly in several weak diffraction peaks, and agreement was obtained only for the equiatomic MgAgAs-type structure. We show the evaluation of the powder diagram of LaPtBi in Table 5.

The final atomic parameters of all structure refinements and the interatomic distances are summarized in Tables 4 and 6. The anisotropic displacement parameters and the structure factor tables have been deposited. They may be obtained from the Fachinformationszentrum Karlsruhe, D-76344 Eggenstein-Leopoldshafen (Germany), by quoting the Registry Numbers: CSD-412360 (TbRhSb), CSD-412362 (SmIrSb), CSD-412359 (SmRhBi), and CSD-412361 (DyRhBi).

TABLE 5
Evaluation of a Guinier Powder Pattern of the Cubic Bismuthide LaPtBi with MgAgAs-Type Structure[a]

d_o (pm)	d_c (pm)	*hkl*	I_o	I_c LaPtBi	I_c "$LaPt_2Bi$"
394.7	394.3	111	30	34	2
341.4	341.5	200	15	10	0.4
241.5	241.4	220	100	100	100
205.9	205.9	311	15	19	1
197.1	197.1	222	2	3	0.1
170.7	170.7	400	20	20	20
156.6	156.7	331	7	9	0.6
152.7	152.7	420	9	5	0.2
139.4	139.4	422	50	47	47
131.4	131.4	511/333	9	8	0.5
120.7	120.7	440	18	19	19

[a] The pattern was recorded with Cu$K\alpha_1$ radiation. The visually estimated intensities I_o are compared with the calculated intensities. For comparison the calculated intensities I_c for a hypothetical compound "$LaPt_2Bi$" with $MnCu_2A1$-type structure are also listed.

DISCUSSION

We have prepared 38 new equiatomic ternary antimonides and bismuthides. Their lattice parameters are listed in Tables 1 and 2 together with the lattice parameters of compounds with similar compositions prepared by other research groups. These compounds are represented in Fig. 1 by their average atomic volumes together with some more compounds from the literature. We have tried to be comprehensive with the literature for the antimonides and bismuthides of the rare earth elements with the transition elements of the ninth and tenth group concerning this figure. However, if a compound has been reported by

TABLE 6
Interatomic Distances in the Equiatomic Compounds TbRhSb, SmIrSb, SmRhBi, and DyRhBi[a]

TbRhSb		SmIrSb		SmRhBi		DyRhBi		PrNiBi	
Tb: 1Rh	307.3	Sm: 1Ir	303.2	Sm: 1Rh	304.1	Dy: 1Rh2	301.9	Pr: 4Ni	281.9
2Rh	311.6	2Sb	315.3	2Bi	321.7	4Rh1	303.9	6Bi	325.6
2Sb	313.0	2Ir	316.2	2Rh	324.9	2Si	320.4	Ni: 4Pr	281.9
1Sb	318.5	1Sb	326.0	1Bi	328.8	4Bi	331.0	4Bi	281.9
2Sb	321.1	2Ir	327.5	2Bi	331.7	2Dy	392.6	Bi: 4Ni	281.9
1Rh	327.9	2Sb	328.9	2Rh	335.9	4Dy	401.7	6Pr	325.6
2Rh	331.6	1Sb	332.1	1Bi	336.4	Rh1: 3Bi	280.9		
1Sb	331.8	1Ir	345.6	1Rh	340.2	6Dy	303.9		
2Tb	364.2	2Sm	371.3	2Sm	372.2	2Rh1	392.6		
2Tb	388.3	2Sm	381.8	2Sm	396.8	Rh2: 6Bi	282.2		
Rh: 2Sb	263.1	Ir: 2Sb	265.8	Rh: 2Bi	270.7	3Dy	301.9		
1Sb	266.4	1Sb	268.1	1Bi	272.8	2Rh2	392.6		
1Sb	278.8	1Sb	278.4	1Bi	289.1	Bi: 2Rh1	280.9		
1Tb	307.3	1Sm	303.2	1Bm	304.1	2Rh2	282.2		
2Tb	311.6	2Sm	316.2	2Sm	324.9	2Dy	320.4		
1Tb	327.9	2Sm	327.5	2Sm	335.9	4Dy	331.0		
2Tb	331.6	1Sm	345.6	1Sm	340.2	2Bi	351.1		
2Rh	378.8	2Ir	397.3	2Rh	401.8	2Bi	392.6		
Sb: 2Rh	263.1	Sb: 2Ir	265.8	Bi: 2Rh	270.7				
1Rh	266.4	1Ir	268.1	1Rh	272.8				
1Rh	278.8	1Ir	278.4	1Rh	289.1				
2Tb	313.0	2Sm	315.3	2Sm	321.7				
1Tb	318.5	1Sm	326.0	1Sm	328.8				
2Tb	321.1	2Sm	328.9	2Sm	331.7				
1Tb	331.8	1Sm	332.1	1Sm	336.4				
2Sb	387.8	2Sb	372.1	2Bi	390.2				

[a] All distances shorter than 430 pm are listed. Standard deviations are all less than 0.3 pm.

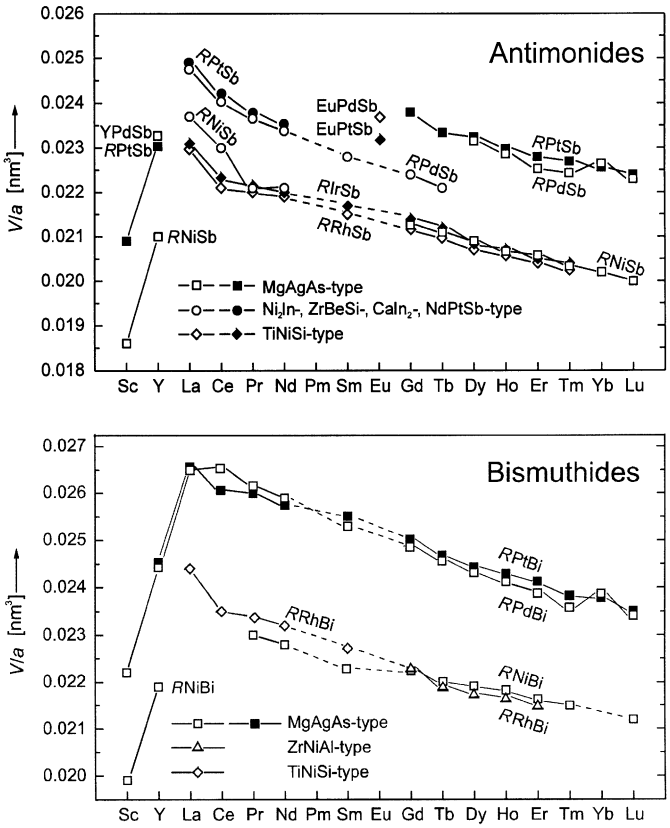

FIG. 1. Average atomic volumes V/a of equiatomic rare earth (R) transition metal (T) antimonides and bismuthides. These plots show the average atomic volumes of compounds listed in Tables 1 and 2 and in addition also average atomic volumes of the compounds with the following references: RNiSb (R = Sc, Y, Gd–Lu) (7), RNiSb (R = La–Nd) (9), RPdSb (R = Y, La–Sm, Gd–Er, Yb) (11), EuPdSb (10), TmPdSb (10), LuPdSb (12), RPtSb (R = Sc, Y, Gd–Lu) (7), RPtSb (R = La–Nd) (13, 14), EuPtSb (15).

several research groups, not all references are cited in Tables 1 and 2, especially if the emphasis was on the physical properties of these compounds and not on the lattice parameters. No equiatomic cobalt-containing compounds have been reported with antimony or bismuth; and up to now, iridium compounds have been found only with antimony as the main group element.

The plots of the average atomic volumes reflect the expected contraction of the trivalent lanthanoids. These plots are not always smooth functions for several reasons. Some of the compounds may have small homogeneity ranges resulting in small ranges of the cell volumes. The compounds were prepared by many different research groups. Some of these were mostly interested in the physical properties of the compounds and paid little attention to the lattice parameters. This may explain why sometimes the average atomic volume of the platinum compound is smaller than that of the corresponding palladium compound, although generally the inverse relationship is observed.

Some of the cerium-containing compounds, i.e., CeRhSb (5, 6), CeIrSb (this work), CeRhBi (6, 19), show small deviations from the smooth functions, indicating a slight admixture of tetravalent cerium. For a larger proportion of tetravalent cerium the cell volumes would need to be smaller than those of the corresponding praseodymium or neodymium compounds. In contrast, the cell volume of CePdBi has been reported to be slightly greater (16) than that found by us for LaPdBi. We have not been successful in preparing that cerium compound. Also, the cell volume of CePtBi reported in ref. (18) is greater than that found by us for the cell volume of the corresponding lanthanum compound LaPtBi. For this reason we have also prepared that cerium compound, where we have observed a smaller cell volume (Table 2), which is plotted in Fig. 1. Thus, the cerium atoms in CePtBi may also be partially tetravalent.

The promethium compounds are all missing, because of the radioactivity of all isotopes of this element. Apparently therefore, it has not been attempted to prepare these compounds, but there is no reason to doubt that the missing promethium compounds could be obtained if the corresponding neodymium and samarium compounds have been synthesized and characterized. This is different for the missing europium compounds, since europium is known to have a tendency for the divalent state and therefore a somewhat different crystal chemistry. Also, europium has a much higher vapor pressure and therefore the europium compounds frequently need to be prepared differently than the corresponding samarium or gadolinium compounds. Figure 1 shows the cell volumes of the two europium antimonides EuPdSb (10) and EuPtSb (15) which crystallize with the orthorhombic TiNiSi-type structure. This structure is also adopted by the seemingly isoelectronic compounds RRhSb (5, this work), RIrSb (this work) with R = La–Nd, Sm, Gd–Tm, and also by CaPtSb (15). Of the ytterbium compounds the ones with palladium, YbPdSb and YbPdBi, show cell volumes which are larger than those of the corresponding thulium compounds. This indicates that ytterbium is partially divalent in these compounds. For the corresponding platinum compounds, YbPtSb and YbPtBi, the cell volumes fit well between those of the thulium and lutetium compounds, thus indicating the ytterbium atoms to be purely trivalent. This difference between the palladium compounds, on the one hand, and the platinum compounds, on the other hand, may be rationalized by the different nobility of these two platinum metals. The more noble platinum atoms have a greater tendency to keep electrons (accommodate them in lower lying states or bands), thus favoring the higher valence of the ytterbium atoms. However, if only the nobility of the transition elements were important, the ytterbium atoms

should have an even larger proportion of Yb^{+2} in YbNiSb, since nickel is even less noble than palladium. As can be seen from the average atomic volumes of the series *R*NiSb (Fig. 1), the ytterbium atoms in these compounds are mostly trivalent. This can be rationalized by the size effect. The polyanionic framework of nickel and antimony atoms is smaller than the frameworks of the corresponding palladium and platinum compounds. This may favor the smaller volume (and higher valence) of the ytterbium atoms in YbNiSb.

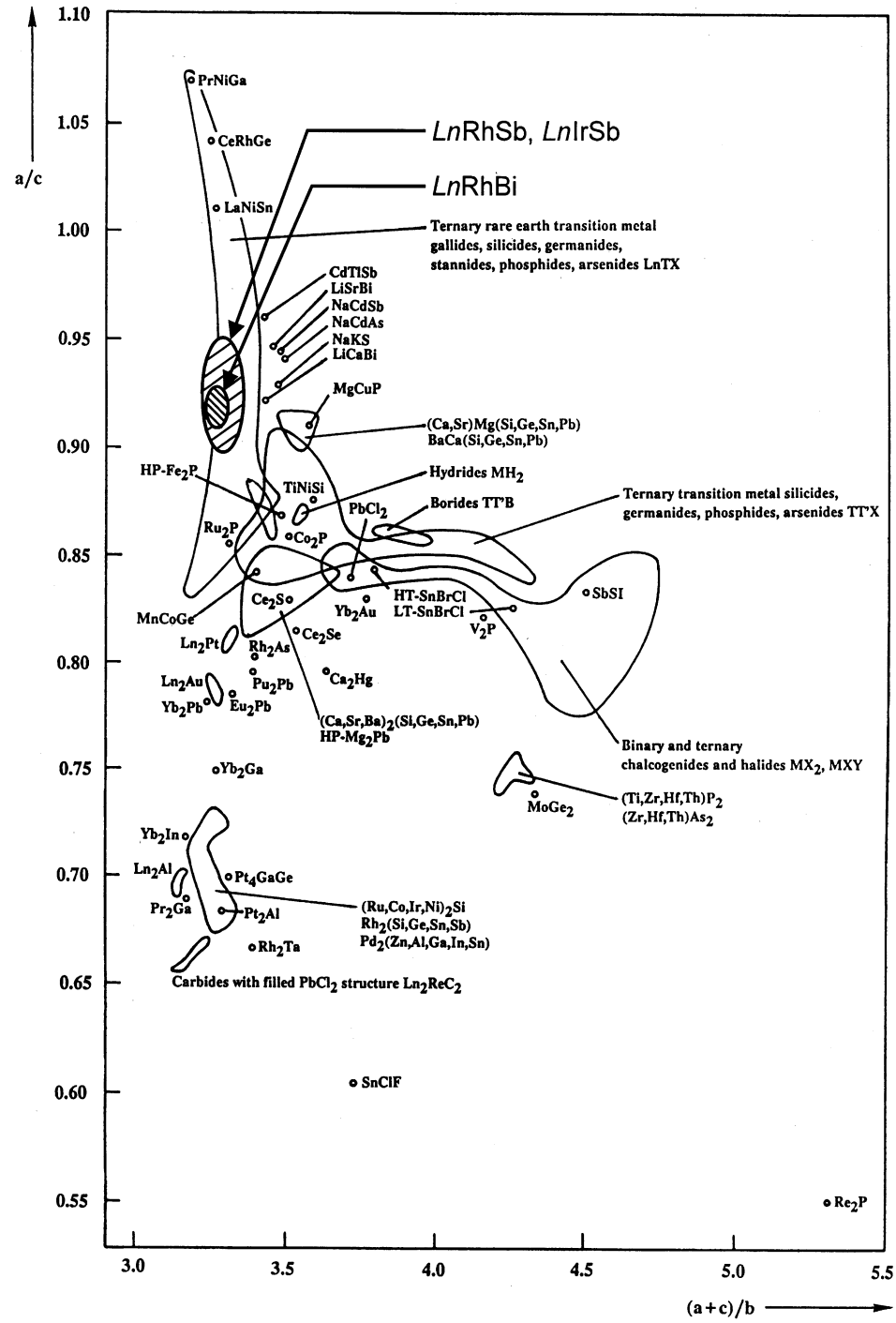

FIG. 2. Axial ratios a/c and $(a+c)/b$ of the new antimonides and bismuthides *Ln*RhSb, *Ln*IrSb, and *Ln*RhBi with the orthorhombic $PbCl_2$-type structure in relation to the axial ratios of other isotypic compounds. Similar diagrams with these axial ratios of $PbCl_2$-type compounds have been published earlier (33–35).

The new compounds reported by us crystallize with three different crystal structures. All of the new antimonides and some of the bismuthides crystallize with the ordered (anti-) $PbCl_2$-type (Co_2Si-type) structure, which frequently is also called the TiNiSi-type structure (32) in the case of ternary compounds with a high metal content. There are many binary and ternary $PbCl_2$-type compounds which formally are all isotypic. However, their near-neighbor coordinations and consequently chemical bonding in these compounds may differ greatly, as can be concluded from the great variety of different axial ratios a/c and $(a+c)/b$. These are plotted in Fig. 2. It can be seen that the axial ratios of the new antimonides and bismuthides *Ln*RhSb, *Ln*IrSb, and *Ln*RhBi fit well into the range of axial ratios of corresponding rare earth transition metal silicides, germanides, stannides, phosphides, and arsenides.

The new bismuthides *Ln*RhBi (*Ln* = Gd–Er) crystallize with the hexagonal ordered Fe_2P-type (36), also called the ZrNiAl-type structure in the case of ternaries (37). Both, the orthorhombic TiNiSi- and the hexagonal ZrNiAl-type structures may be regarded as derived from the most simple $A1B_2$-type structure (38). Both of these structures are shown in Fig. 3 in projections along the short translation period. In both structures all atoms are situated at two mirror planes which extend perpendicular to the short translation period. The atoms situated at these two mirror planes are connected by thick and thin lines to facilitate their visualization. These lines do not necessarily represent strong chemical bonds. Also, these structures should not be regarded as layered structures, since chemical bonding within and between the layers is of comparable strength, as can be gathered from the coordination polyhedra shown in Fig. 4. Both of these structure types may be regarded as very simple representatives of a large family of structures with a metal:nonmetal ratio of 2:1 (39–43). The nonmetal atoms are usually main group elements in the vicinity of the Zintl border (e.g., the elements boron, silicon, phosphorus, and their homologues). These structures are frequently classified by the kind of linking of the trigonal prisms (usually) surrounding the nonmetal atoms. These trigonal prisms are emphasized in the lower part of Fig. 3. However, in the case of the ZrNiAl-type structure of DyRhBi the trigonal prisms are centered by the rhodium atoms. Actually, there is a transition for the occupancy of the sites centered by the trigonal prisms in going from compounds with light metalloid atoms to compounds with

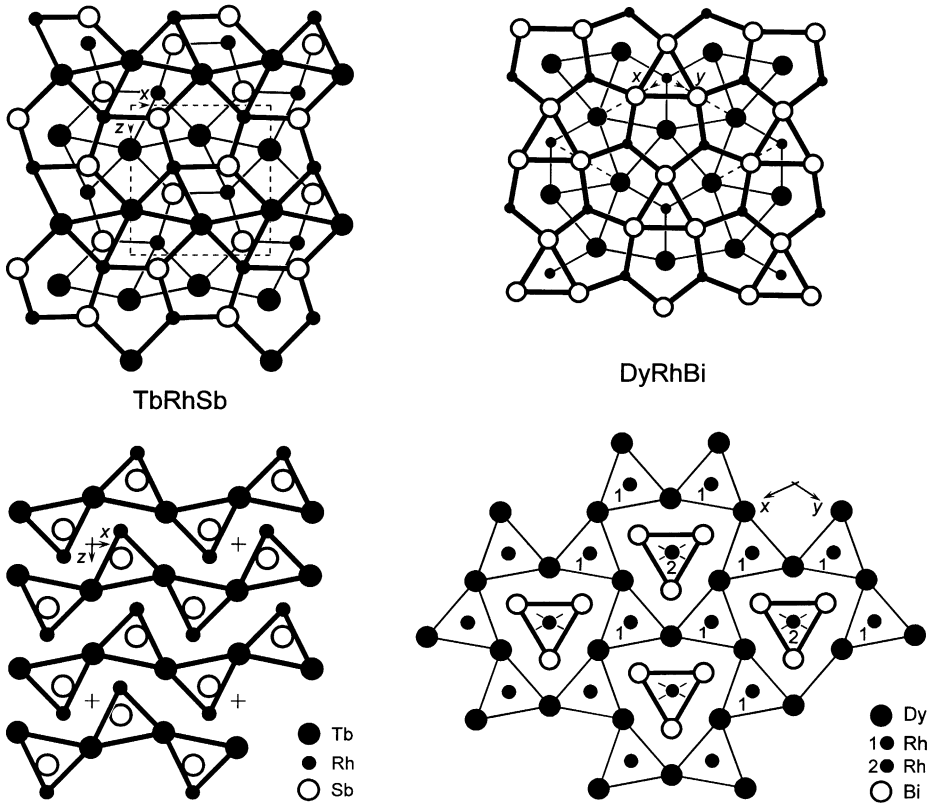

FIG. 3. Crystal structures of orthorhombic TbRhSb (TiNiSi-type) and hexagonal DyRhBi (ZrNiAl-type). The structures are projected along the short tanslation periods. In the upper part of the figure atoms at the same heights are connected by thick and thin lines, respectively. In the lower part the trigonal prisms surrounding the antimony and rhodium atoms are emphasized.

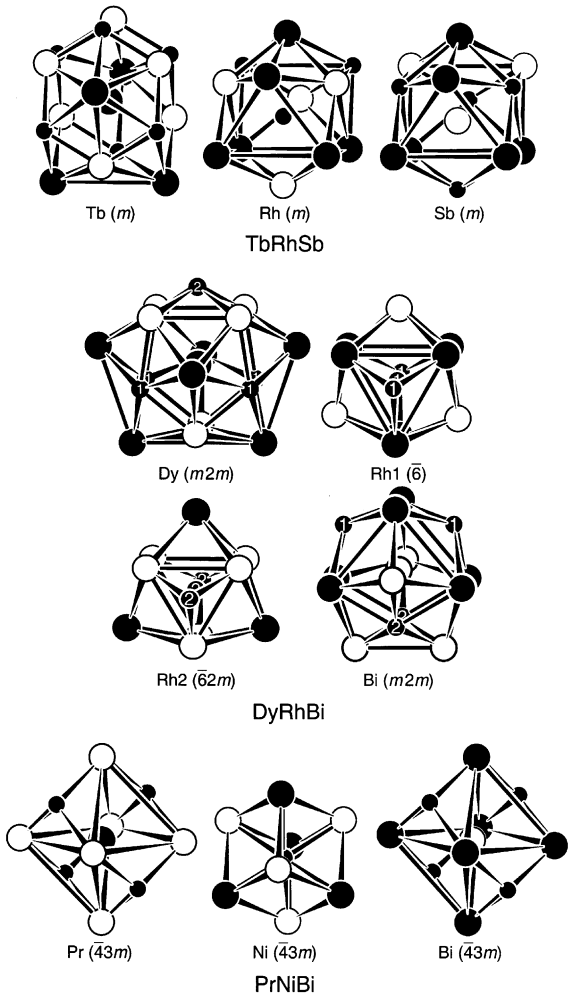

FIG. 4. Coordination polyhedra in the structures of TbRhSb (orthorhombic TiNiSi-type), DyRhBi (hexagonal ZrNiAl-type), and cubic MgAgAs-type PrNiBi. All near neighbors as listed in Table 5 are shown.

the heavy metalloids. We will demonstrate this with the following examples. In the ternary compounds with metalloids and metals of the third main group of the Periodic System (B, Al, Ga, In, Tl) the boron atoms in NbFeB (44) occupy the Wyckoff positions 2*d* and 1*a* of the ZrNiAl-type structure (standardized setting, see Table 4), while these positions are occupied by the late transition metal atoms in the isotypic aluminum, gallium, indium, and thallium compounds ZrNiAl (37), CeNiAl (45), URhAl (46), UNiGa (47), YNiIn (48), DyNiIn (48), CePdIn (48), and in the series *Ln*PdTl (*Ln* = Y, La–Nd, Sm, Gd–Er, Yb) (49). The silicon and the germanium atoms in NbMnSi (50) and TiCoGe (51) occupy the 2*d* and 1*a* positions of the ZrNiAl-type structure, whereas in the stannides HoPtSn (52), α-YbPdSn (53), and YbPtSn (54) as well as in the plumbide YPdPb (55) these sites are occupied by the platinum metal atoms. Finally, with the pnictides, the phosphorus and arsenic atoms in the ternary compounds ScRuP (56), *T*RuP (*T* = Ti, Zr, Hf) (57), ZrRuAs (58), and YbPdAs (59) occupy the 2*d* and 1*a* positions of the ZrNiAl-type structure, while in the ternary bismuthides *Ln*RhBi, reported in the present paper, these sites are occupied by the rhodium atoms, as is clearly demonstrated by the structure refinement of DyRhBi. Obviously, this transition in the occupancy of the 2*d* and 1*a* sites on the one hand, and the 3*g* site on the other hand, has to do with the space requirements of the metalloid atoms as they become larger. The relatively large Al, Ga, Tl, Sn, Pb, and Bi atoms prefer the 3*g* site, since this site offers the higher coordination number CN of 12 *vs.* CN 9 for the sites 2*d* and 1*a* which are preferred by the B, Si, Ge, P, and As atoms. Such a change does not occur for the orthorhombic TiNiSi-type structure, where the positional parameters can change gradually to accommodate large or small atoms on the nickel and silicon positions, thereby also changing the CNs of these positions. Thus, the boron atoms of the TiNiSi-type structure of MoCoB have nine near neighbors (33), while the antimony and bismuth atoms of the presently refined structures of TbRhSb, SmIrSb, and SmRhBi, on the same sites as the boron atoms in MoCoB, have 10 near neighbors. It can be seen from the drawing in the lower left-hand part of Fig. 3 that the antimony atoms in TbRhSb are not occupying the centers of their trigonal prisms. They have moved off the center, thus approaching a Tb atom (with a Sb–Tb distance of 331.8 pm) as tenth neighbor. In Table 6 and in Fig. 4 the antimony atoms are listed and shown, respectively, with two more antimony neighbors, thus increasing their CN to 12. However, the corresponding Sb–Sb distances of 387.8 pm (in TbRhSb) are rather large and at best these interactions may be considered as only very weakly bonding (60).

Finally, in the course of the present work we have found several equiatomic cubic compounds with the very simple MgAgAs-type structure (Fig. 5) which has only the lattice parameter as a structural variable. Of the 21 bismuthides

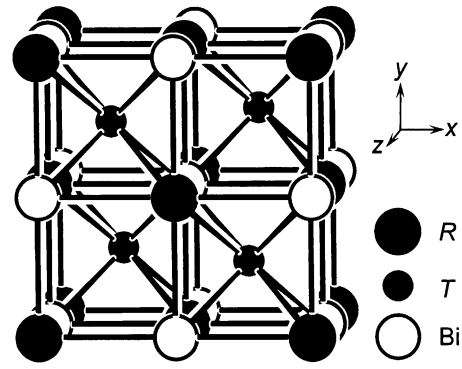

FIG. 5. Cubic MgAgAs-type structure of the rare earth (*R*) transition metal (*T*) bismuthides *RT*Bi.

with MgAgAs-type structure prepared by us (Table 2) the 12 compounds *Ln*NiBi (*Ln* = Pr, Nd, Sm, Tb, Ho, Er), *Ln*PdBi (*Ln* = Sc, La, Er, Tm, Lu), and LaPtBi are reported here for the first time. The compounds *Ln*PtBi (*Ln* = Y, Nd, Gd, Tb, Dy) are small-gap semiconductors or semimetals (18) and this can also be expected for the structurally isotypic and isoelectronic bismuthides reported by us.

ACKNOWLEDGMENTS

We thank Dipl.-Ing. U. Ch. Rodewald for the data collections on the four-circle diffractometer and Mr. H.-J. Göcke for the work at the scanning electron microscope. We are also indebted to Dr. W. Gerhartz (Degussa) and Dr. G. Höfer (Heraeus Quarzschmelze, Hanau) for generous gifts of rhodium powder and silica tubes, respectively. This work was also supported by the Deutsche Forschungsgemeinschaft, the Fonds der Chemischen Industrie, and the International Centre for Diffraction Data.

REFERENCES

1. P. Villars, *J. Less-Common Met.* **119,** 175 (1986).
2. E. Hovestreydt, *J. Less-Common Met.* **143,** 25 (1988).
3. R. Pöttgen and D. Johrendt, *Chem. Mater.* **12,** 875 (2000).
4. R. Pöttgen, D. Johrendt, and D. Kußmann, *in* "Handbook on the Physics and Chemistry of Rare Earths" (K. A. Gschneidner Jr., L. Eyring, and G. H. Lander, Eds.), Vol. 32, pp. 453–513, North-Holland, Amsterdam, 2001.
5. S. K. Malik and D. T. Adroja, *Phys. Rev. B* **43,** 6277 (1991).
6. P. Salamakha, O. Sologub, T. Suemitsu, and T. Takabatake, *J. Alloys Compd.* **313,** L5 (2000).
7. A. E. Dwight, *in* "Proceedings of Rare Earth Research Conference 11th" (J. M. Haschke and H. A. Eick, Eds.), pp. 642–650, NTIS, Springfield, VA, 1974.
8. K. Hartjes and W. Jeitschko, *J. Alloys Compd.* **226,** 81 (1995).
9. I. Karla, J. Pierre, and R. V. Skolozdra, *J. Alloys Compd.* **265,** 42 (1998).
10. S. K. Malik and D. T. Adroja, *J. Magn. Magn. Mater.* **102,** 42 (1991).
11. R. Marazaa, D. Rossi, and R. Ferro, *J. Less-Common Met.* **75,** P25 (1980).
12. K. Mastronardi, D. Young, C.-C. Wang, P. Khalifah, and R. J. Cava, *Appl. Phys. Lett.* **74,** 1415 (1999).
13. D. Rossi, R. Marazza, D. Mazzone, and R. Ferro, *J. Less-Common Met.* **78,** P1 (1981).
14. G. Wenski and A. Mewis, *Z. Kristallogr.* **176,** 125 (1986).
15. G. Wenski and A. Mewis, *Z. Anorg. Allg. Chem.* **543,** 49 (1986).
16. R. Marazza, D. Rossi, and R. Ferro, *Gazz. Chim. Ital.* **110,** 357 (1980).
17. P. Riani, D. Mazzone, G. Zanicchi, R. Marazza, and R. Ferro, *Z. Metallkd.* **86,** 450 (1995).
18. P. C. Canfield, J. D. Thompson, W. P. Beyermann, A. Lacerda, M. F. Hundley, E. Peterson, Z. Fisk, and H. R. Ott, *J. Appl. Phys.* **70,** 5800 (1991).
19. S. Yoshii, D. Tazawa, and M. Kasaya, *Physica B* **230–232,** 380 (1997).
20. H. Block, T. Wölpl, and W. Jeitschko, *Acta Crystallogr. A* **46,** C-290 (1990).
21. T. Schmidt and W. Jeitschko, *Z. Kristallogr. Suppl.* **17,** 123 (2000).
22. M. Haase and W. Jeitschko, *Z. Kristallogr. Suppl.* **17,** 124 (2000).
23. K. Yvon, W. Jeitschko, and E. Parthé, *J. Appl. Crystallogr.* **10,** 73 (1977).
24. B. A. Frenz and Associates Inc. and Enraf-Nonius. SDP (Structure Determination Package), Version 3, College Station (Texas) and Delft (Holland), 1985.
25. G. M. Sheldrick, SHELXL-97, a Computer Program System for Crystal Structure Refinement. University of Göttingen, Germany, 1997.
26. L. M. Gelato and E. Parthé, *J. Appl. Crystallogr.* **20,** 139 (1987).
27. H. D. Flack, *Acta Crystallogr. A* **39,** 876 (1983).
28. G. Bernardinelli and H. D. Flack, *Acta Crystallogr. A* **41,** 500 (1985).
29. H. Nowotny and W. Sibert, *Z. Metallkd.* **33,** 391 (1941).
30. Ch. B. H. Evers, C. G. Richter, K. Hartjes, and W. Jeitschko, *J. Alloys Compd.* **252,** 93 (1997).
31. W. Jeitschko, *Met. Trans.* **1,** 3159 (1970).
32. C. B. Shoemaker and D. P. Shoemaker, *Acta Crystallogr.* **18,** 900 (1965).
33. W. Jeitschko, *Acta Crystallogr. B* **24,** 930 (1968).
34. W. Jeitschko and R. O. Altmeyer, *Z. Naturforsch.* **45b,** 947 (1990).
35. W. Jeitschko, G. Block, G. E. Kahnert, and R. K. Behrens, *J. Solid State Chem.* **89,** 191 (1990).
36. S. Rundqvist and F. Jellinek, *Acta Chem. Scand.* **13,** 425 (1959).
37. P. I. Krypyakevich, V. Ya. Markiv, and Ya. V. Melnyk, *Dopov. Akad. Nauk Ukr. RSR A* **29,** 750 (1967).
38. R.-D. Hoffmann and R. Pöttgen, *Z. Krostallogr.* **216,** 127 (2001).
39. R. Madar, V. Ghetta, E. Dhahri, P. Chaudouët, and J. P. Senateur, *J. Solid State Chem.* **66,** 73 (1987).
40. E. Parthé and B. Chabot, *in* "Handbook on the Physics and Chemistry of Rare Earths," (K. A. Gschneidner Jr. and L. Eyring, Eds.), Vol. 6, pp. 113–334, North-Holland, Amsterdam, 1984.
41. Yu. B. Kuz'ma and S. Chykhrij, *in* "Handbook on the Physics and Chemistry of Rare Earths," (K. A. Gschneidner Jr. and L. Eyring, Eds.), Vol. 23, pp. 285–434, North-Holland, Amsterdam, 1996.
42. J.-Y. Pivan and R. Guérin, *J. Solid State Chem.* **135,** 218 (1998).
43. Yu. M. Prots' and W. Jeitschko, *Inorg. Chem.* **37,** 5431 (1998).
44. Yu. B. Kuz'ma, *Dopov. Akad. Nauk Ukr. RSR. A* **29,** 939 (1967).
45. A. E. Dwight, M. H. Mueller, R. A. Conner Jr., J. W. Downey, and H. Knott, *Trans. Amer. Inst. Min. (Metall.) Engrs.* **242,** 2075 (1968).
46. J. A. Paixão, G. H. Lander, P. J. Brown, H. Nakotte, F. R. de Boer, and E. Brück, *J. Phys. Condens. Matter* **4,** 829 (1992).
47. H. Maletta, R. A. Robinson, A. C. Lawson, V. Sechovskỳ, L. Havela, L. Jirman, M. Divis, E. Brück, F. R. de Boer, A. V. Andreev, K. H. J. Buschow, and P. Burlet, *J. Magn. Magn. Mater.* **104–107,** 21 (1992).
48. R. Ferro, R. Marazza, and G. Rambaldi, *Z. Metallkd.* **65,** 37 (1974).
49. R. Ferro, R. Marazza, and G. Rambaldi, *Z. Metallkd.* **65,** 40 (1974).
50. B. Deyris, J. Roy-Montreuil, R. Fruchart, and A. Michel, *Bull. Soc. Chim. Fr.* **1968,** 1303 (1968).
51. W. Jeitschko, *Acta Crystallogr. B* **26,** 815 (1970).
52. A. E. Dwight, W. C. Harper, and C. W. Kimball, *J. Less-Common Met.* **30,** 1 (1973).
53. D. Kußmann, R. Pöttgen, B. Künnen, G. Kotzyba, R. Müllmann, and B. D. Mosel, *Z. Kristallogr.* **213,** 356 (1998).
54. R. Pöttgen, A. Lang, R.-D. Hoffmann, B. Künnen, G. Kotzyba, R. Müllmann, B. D. Mosel, and C. Rosenhahn, *Z. Kristallogr.* **214,** 143 (1999).
55. A. Iandelli, *J. Alloys Compd.* **203,** 137 (1994).
56. V. Ghetta, P. Chaudouët, B. Lambert-Andron, M.-N. Deschizeaux-Cheruy, R. Madar, and J.-P. Senateur, *C. R. Acad. Sci. Paris, Ser. II,* **303,** 357 (1986).
57. G. P. Meisner and H. C. Ku, *Appl. Phys. A* **31,** 201 (1983).
58. G. P. Meisner, H. C. Ku, and H. Barz, *Mater. Res. Bull.* **18,** 983 (1983).
59. D. Johrendt and A. Mewis, *J. Alloys Compd.* **183,** 210 (1992).
60. W. Jeitschko, R. O. Altmeyer, M. Schelk, and U. Ch. Rodewald, *Z. Anorg. Allg. Chem.* **627,** 1932 (2001).